

Analytical solution for clay plug swelling experiments

Simon A. Mathias^{a,*}, H. Chris Greenwell^a, Charlotte Withers^a, Ali R. Erdogan^a, Jim N. McElwaine^a, Chris MacMinn^b

^a*Department of Earth Sciences, Durham University, Durham, UK*

^b*Department of Engineering Science, Oxford University, Oxford, UK*

Abstract

Clay swelling experiments frequently involve monitoring the one-dimensional displacement with time of an initially dry clay plug as it imbibes water from a supply at its base. This article presents a new analytical solution for interpreting such experiments based on Richards' equation for flow in a partially saturated porous medium combined with a linear empirical function relating moisture ratio with void ratio. The analytical solution is described by just two parameter groups. The first parameter group describes the swelling potential of the clay. The second parameter group describes the rate at which the swelling plug reaches equilibrium, which is controlled by permeability and capillary pressure. Application of the analytical solution is demonstrated by calibration to one-dimensional displacement data from clay swelling experiments for an illite and bentonite clay.

Keywords: Swelling, Unsaturated, Clay, Diffusion, Absorption, Richards' equation

1. Introduction

Compacted Wyoming bentonite, a clay rock composed predominantly of sodium montmorillonite, is widely used as a barrier material for nuclear radioactive waste repositories, as an adsor-

*Corresponding author. Tel.: +44 (0)1913343491, Fax: +44 (0)1913342301, E-mail address: s.a.mathias@durham.ac.uk

11 bent, and as an analogue for swelling clay mineral rich sub-sea shale formations (Komine & Ogata,
12 1994). The two-dimensional layered structure of aluminosilicate clay minerals results in a high
13 surface area and, combined with the presence of exchangeable cations, gives rise to the adsorbent
14 properties of bentonite for radionuclides (for example, Cs⁺), and other contaminants (Eriksen et
15 al., 1999).

16 These properties of bentonite and related clay minerals also result in a propensity to sponta-
17 neously hydrate upon contact with water. To accommodate this hydration, the bulk volume of the
18 clay mineral must increase if the material is unconfined; if confined, a swelling pressure arises
19 instead. Upon swelling, the transport properties of the hydrated clay mineral material also change
20 due to the changes in pore size distribution.

21 One manifestation of swelling that presents significant challenges to oil and gas operations
22 is shale instability. Oil and gas reservoirs are usually topped by an impervious cap rock, which
23 holds the less dense hydrocarbons within the subterranean reservoir. In most cases, the caprock
24 will be a clay mineral rich shale. Thus shales are invariably encountered when drilling the well-
25 bore to access the oil reservoir. To clear the rock fragments (cuttings) from the well-bore during
26 drilling, and to maintain hydrostatic pressure in the cleared hole and thus formation integrity, a
27 technical drilling fluid is used. This fluid is colloquially known as “mud”. In the early days
28 of oil exploration, oil-based muds (OBM) were generally used, based on crude oil. However,
29 owing to the environmental impacts of OBMs, drilling engineers have focussed on developing less
30 environmentally damaging water-based muds (WBM).

31 The clay minerals present in shale may either disperse (for example kaolinite) or swell (for
32 example montmorillonite) upon contact with WBMs, causing instability in the well bore region,

33 such as swelling/sloughing, in the medium-long term, or increased plasticity and the aggrega-
34 tion of shale cuttings to the drill string (“bit balling”) in the short term (Anderson et al., 2010).
35 The swelling of clay is strongly controlled by the composition of pore-water (Chai et al., 2014;
36 Chen, 2016; Chavali et al., 2017; Oren and Akar, 2017). To address these problems, the industry
37 has tried to increase the environmental performance of WBMs through use of more sophisticated
38 water-based technologies including small organic molecules to inhibit clay mineral/shale swelling.
39 Compacted bentonite is frequently used as a model in which to probe the efficacy of the swelling
40 inhibitors.

41 The swelling properties of clay minerals have long been studied, in aqueous brines and in
42 organic solvents (Anderson et al., 2010), though often at the single crystal level. Clay crystal
43 swelling has been partitioned into both crystalline and osmotic swelling regimes (Anderson et al.,
44 2010). Studies have primarily focussed on the equilibrium swelling of the clay minerals, with the
45 expansion of the crystal at given conditions of temperature and salinity tested against classical
46 colloid theories, e.g. DLVO theory (Smalley, 2006). Though the crystal chemistry and swelling
47 potential of clay minerals are relatively well understood (Wilson & Wilson, 2014; Anderson et al.,
48 2010), the link between clay mineral crystal swelling and shale stability, where many components
49 influence the bulk swelling (Van Oort, 2003), is less clear, and it has even been argued that clay
50 mineral swelling properties are not relevant in the oil field and that shale swelling may not occur
51 when artefacts of experiments are carefully accounted for (Santarelli & Carminati, 1995).

52 It is inherently challenging to create compacted shale-like materials that replicate the proper-
53 ties and behaviour of saturated shale under wellbore conditions. As such, compacted bentonite
54 and other natural clays will remain in use as a proxy for shales to allow testing of drilling fluid

55 formations and additives and it is imperative to account for the artefacts introduced during produc-
56 tion of compacted clay mineral shale analogues to be able to discern performance improvements
57 in new drilling fluid technologies (Santarelli & Carminati, 1995). In particular, and especially to
58 attempt to understand bit balling, the short term swelling rates of clay minerals need to be better
59 understood.

60 To address this, a non-contact one-dimensional displacement meter has been developed and
61 used to measure the short term swelling response of compacted bentonite tablets (Sellick et al.,
62 2017). Similar experiments in this context are also reported by Chen (2016). Modelling of the
63 swelling process can help reveal the relative importance of processes contributing to the compacted
64 bentonite swelling. Whereas very accurate computational chemistry methods, such as atomistic
65 molecular dynamics, have enabled swelling energetics to be probed at the clay mineral crystal
66 scale (Suter et al., 2011), and more complex multi-scale methods have been developed (Suter
67 et al., 2015), these are computationally very expensive. The objective of this study is to improve
68 understanding about the kinetics of hydration processes through an analytical model, which allows
69 rapid calculation of swelling curves to be tested against experimental data.

70 Our approach builds on modeling techniques previously developed to understand swelling and
71 shrinkage of clay rich soils (Philip, 1969; Smiles and Raats, 2005; Su, 2010). Such models em-
72 ploy Richards' equation to describe water movement through partially saturated porous media
73 combined with empirical relationships between moisture ratio (volume of water / total volume)
74 and void ratio (volume of voids / total volume) (Peng and Horn, 2007). The swelling of clay gives
75 rise to moving boundary conditions. However, these can be dealt with by using a material coordi-
76 nate system, associated with a theoretical dry clay mass, as opposed to a spatial coordinate system

77 (Philip, 1969; Su, 2010).

78 In the context of the swelling experiments described above, the resulting non-linear partial dif-
79 ferential equation (PDE) have traditionally been solved numerically using finite differences (Kim,
80 1999). Although a range of analytical and quasi-analytical solutions for this class of problem have
81 been sought in the past (Raats, 2002), these have mostly been in the context of infiltration. In
82 this article, a linear relationship between moisture ratio and void ratio is assumed such that the
83 resulting PDE is linear and can be solved analytically. An exact analytical solution for the one-
84 dimensional displacement of a compacted clay tablet as a function of time is then derived. Finally,
85 the efficacy of the analytical solution is demonstrated by calibration to experimental data sets from
86 two different clays.

87 **2. Mathematical model**

88 The approach used here was originally developed by Philip (1969) in the context of swelling
89 soils, and has been frequently applied in the context of soil-deformation modeling (Kim, 1999;
90 Smiles and Raats, 2005; Su, 2010). An explanation of how this approach can be used to derive an
91 analytical solution for clay plug swelling experiments is described as follows.

92 The bulk volume of an unsaturated clay mass, V_b [L^3], can be defined by

$$V_b = V_w + V_c + V_a \quad (1)$$

93 where V_w [L^3], V_c [L^3] and V_a [L^3] are the volumes of water (including free and adsorbed water),
94 clay mineral (excluding all water) and air present within the bulk clay mass of concern, respec-

95 tively.

96 The swelling of clay due to the presence of water manifests itself through a strong correlation
97 between void ratio, e [-], and moisture ratio, ϑ (e.g. Peng and Horn, 2007; Chertkov, 2012), defined
98 by:

$$e = \frac{V_w + V_a}{V_c} \quad (2)$$

99

$$\vartheta = \frac{V_w}{V_c} \quad (3)$$

100 A simple way to represent this correlation is to assume that e and ϑ are related by the linear
101 function

$$e = e_I + (\vartheta_s - e_I) \left(\frac{\vartheta - \vartheta_I}{\vartheta_s - \vartheta_I} \right) \quad (4)$$

102 where e_I [-], ϑ_I [-] and ϑ_s [-] represent the initial void ratio, initial moisture ratio and maximum
103 moisture ratio of a clay sample, respectively.

104 Consider water movement through the bulk clay associated with a mineral clay volume of δV_c .
105 Let δQ [L^3T^{-1}] be the net rate of out-flowing water. Assuming the water and mineral clay to be
106 incompressible, the change in moisture ratio, $\delta\vartheta$, over a a time-period, δt [T], is found from

$$\delta\vartheta\delta V_c = -\delta Q\delta t \quad (5)$$

107 such that for an infinitesimal time-period and mineral clay volume

$$\frac{\partial\vartheta}{\partial t} = -\frac{\partial Q}{\partial V_c} \quad (6)$$

108 *2.1. One-dimensional vertical flow*

109 Now consider a vertically oriented cylindrical clay plug encased within a rigid and imperme-
 110 able sleeve. The clay is initially dried to a uniform moisture ratio, ϑ_I , and uniform void ratio, e_I .
 111 The base of the clay plug is then soaked in water at a fixed pressure whilst the top of the plug is
 112 exposed to the atmosphere. In this way, the volumetric flow rate of water, Q , can be assumed to
 113 be described by the following form of Darcy's law (Philip, 1969)

$$Q = -\frac{Akk_r}{\mu_w} \frac{\partial(P_w + \rho_w gz + P_o)}{\partial z} \quad (7)$$

114 where A [L^2] is the cross-sectional area of the clay plug (which is constant due to the rigid sleeve),
 115 k [L^2] is the permeability, k_r [-] is relative permeability (which is a function of ϑ), P_w [$ML^{-1}T^{-2}$]
 116 is water pressure, μ_w [$ML^{-1}T^{-1}$] is the dynamic viscosity of water, ρ_w [ML^{-3}] is the density of
 117 water, g [LT^{-2}] is gravitational acceleration, z [L] is elevation and P_o [$ML^{-1}T^{-2}$] is the so-called
 118 overburden pressure associated with the work done in swelling the clay. See Raats (2002) for
 119 further discussion with regards to the overburden pressure term.

120 Capillary pressure, P_c [$ML^{-1}T^{-2}$], is defined by $P_c = P_a - P_w$ where P_a [$ML^{-1}T^{-2}$] is the air
 121 pressure. Importantly, capillary pressure is a function of ϑ . Analogous to Richards' equation,
 122 assuming the air pressure to be constant throughout and capillary pressure variations to be much
 123 larger than those associated with gravity head and overburden pressure (which is very likely in
 124 clay media), Eq. (7) reduces to

$$Q = \frac{Akk_r}{\mu_w} \frac{\partial P_c}{\partial \vartheta} \frac{\partial \vartheta}{\partial z} \quad (8)$$

125 The relevant initial and boundary conditions are:

$$\begin{aligned}\vartheta &= \vartheta_I, & 0 \leq z \leq H_I, & t = 0 \\ \vartheta &= \vartheta_s, & z = 0, & t > 0 \\ Q &= 0, & z = H(t), & t > 0\end{aligned}\tag{9}$$

126 where H_I [L] is the initial height of the clay plug and $H(t)$ [L] is the height of the clay plug at time,
127 t . Note that the height of the clay plug increases with time as the clay plug swells due to water
128 adsorption within the clay layers.

129 2.2. Transformation to a static boundary condition

130 Considering Eqs. (1) and (2), the relationship between V_c and z is defined by

$$\frac{\partial V_c}{\partial z} = \frac{A}{e + 1}\tag{10}$$

131 Let us now consider an alternative coordinate, ζ [L], defined by

$$\frac{\partial V_c}{\partial \zeta} = \frac{A}{e_I + 1}\tag{11}$$

132 It can be understood that

$$\frac{\partial \zeta}{\partial z} = \frac{e_I + 1}{e + 1}\tag{12}$$

133 and furthermore that

$$H(t) = \int_0^{H_I} \frac{e + 1}{e_I + 1} d\zeta\tag{13}$$

134 Eqs. (6), (8) and (9) map to the ζ coordinate system to form a non-linear diffusion problem as
 135 follows:

$$\frac{\partial \vartheta}{\partial t} = \frac{\partial}{\partial \zeta} \left(D_A(\vartheta) \frac{\partial \vartheta}{\partial \zeta} \right) \quad (14)$$

136

$$\begin{aligned} \vartheta &= \vartheta_I, & 0 \leq \zeta \leq H_I, & t = 0 \\ \vartheta &= \vartheta_s, & \zeta = 0, & t > 0 \\ Q &= 0, & \zeta = H_I, & t > 0 \end{aligned} \quad (15)$$

137 where D_A [L^2T^{-1}] is the apparent diffusion coefficient, defined by

$$D_A = - \frac{(e_I + 1)^2 k k_r}{(e + 1) \mu_w} \frac{\partial P_c}{\partial \vartheta} \quad (16)$$

138 The above set of equations can also be derived using the large deformation mathematical
 139 framework of Song & Borja (2014).

140 2.3. Analytical solution for linear diffusion coefficient

141 For the special case when D_A can be treated as a positive constant, the above problem has an
 142 analytical solution of the form (similar to Crank, 1975, p. 47)

$$\frac{\vartheta - \vartheta_I}{\vartheta_s - \vartheta_I} = 1 - 2 \sum_{n=0}^{\infty} \frac{1}{\lambda_n} \exp\left(-\frac{\lambda_n^2 D_A t}{H_I^2}\right) \sin\left(\frac{\lambda_n \zeta}{H_I}\right) \quad (17)$$

143 where $\lambda_n = (n + 1/2)\pi$.

144 Substituting Eq. (17) into Eq. (4) and then into Eq. (13) leads to

$$h(t) = \alpha \left[1 - 2 \sum_{n=0}^{\infty} \frac{1}{\lambda_n^2} \exp(-\beta \lambda_n^2 t) \right] \quad (18)$$

145 where

$$h(t) = \frac{H - H_I}{H_I}, \quad \alpha = \frac{\vartheta_s - e_I}{e_I + 1}, \quad \beta = - \left(\frac{e_I + 1}{H_I} \right)^2 \frac{kk_r}{(e + 1)\mu_w} \frac{\partial P_c}{\partial \vartheta} \quad (19)$$

146 and $h(t)$ [-] is hereafter referred to as the swelling ratio. Note that this is the first and only time
147 that the linear relationship between e and ϑ (Eq. (4)) is invoked.

148 For a zero e_I , $\alpha = \vartheta_s$. The α parameter says something about the adsorption capacity of the
149 clay. Higher values of α imply greater adsorption potential and hence greater swelling potential.
150 The β parameter represents the rate at which a clay swelling experiment equilibrates. Large values
151 of β correspond to high permeability and/or high capillary pressures. Large β values lead to the
152 clay reaching equilibrium faster.

153 3. Calibration to experimental data

154 Artificial cylindrical plugs of clay were processed with a thickness of 3.8 mm and a diameter
155 of 20 mm. The clay plugs were placed into circular sample holders with the base exposed to
156 a water bath. Clay plugs within the sample holders sat on top of circular perforated disks to
157 enable hydraulic contact between the water bath and the base of the plugs. The sample holder
158 was also designed to constrain the plug laterally such that swelling only occurs in the vertical
159 direction. Vertical displacement of the upper surface of the clay plug was measured using an
160 induction sensor non-contact one-dimensional displacement meter. The displacement of the upper

161 surface in the course of time was monitored. Two clay plugs were examined comprised of illite
162 and bentonite. Using illite and bentonite (predominantly sodium montmorillonite) provide near
163 end members in terms of clay swelling response in terms of crystalline swelling. Assuming similar
164 particle size/void space, the additional swelling of any other minerals should fall between or close
165 to these materials.

166 Values of α [-] and β [T^{-1}] were obtained by calibrating Eq. (18) to the observed data. Calibra-
167 tion was achieved by minimizing the mean absolute error (MAE) between observed and simulated
168 h using MATLAB's local optimization routine, FMINSEACH. A comparison of observed and cal-
169 ibrated model results are presented in Fig. 1. The associated calibrated parameters and MAE are
170 presented in Table 1. It is clear that the two parameter analytical solution is capable of catching
171 almost all aspects of the data presented

172 Consider again Eq. (19). The fact that α is larger for bentonite than for illite suggests that
173 bentonite has a larger ϑ_s and hence a greater potential for water adsorption. The fact that β is
174 larger for illite as compared to bentonite suggests that illite has a higher permeability and/or a
175 higher capillary pressure, leading to faster capillary suction of water.

176 **4. Conclusions**

177 The objective of this study was to develop an analytical solution to aid interpretation of one-
178 dimensional displacement observations from clay swelling experiments. An appropriate math-
179 ematical model was developed by combining Richards' equation for flow in partially saturated
180 porous media with a linear empirical function relating void ratio with moisture ratio. By ignoring
181 gravity and overburden pressure and assuming a constant relative permeability and moisture ratio

Table 1: Model calibration results.

Clay type	α (%)	β (hour ⁻¹)	MAE (%)
Illite	44.4	10.1	0.747
Bentonite	70.1	1.06	0.794

182 - capillary pressure ratio, the associated non-linear partial differential equation reduced to a linear
 183 diffusion equation for the water ratio. Making use of Crank (1975), an analytical Fourier series
 184 solution for the water ratio in the swelling clay plug was found. This solution was substituted into
 185 the linear void ratio–moisture ratio function to obtain an expression for the void ratio, which in
 186 turn was used to calculate the height of the sample in the course of time.

187 The analytical solution reveals that one-dimensional displacement is controlled by two impor-
 188 tant parameter groups, α and β (recall Eq. (19)). The α parameter is linked to the maximum mois-
 189 ture ratio for the clay. Large α values imply higher potential for water adsorption and swelling.
 190 The β parameter is linked to permeability and capillary pressure and represents the rate at which a
 191 clay swelling experiment reaches equilibrium.

192 The analytical solution was successfully calibrated to experimental data for two very different
 193 clays: illite and bentonite. The illite was found to have a lower swelling potential (low α) but
 194 was found to equilibrate relatively quickly (high β). In contrast, the bentonite was found to have a
 195 much greater swelling potential (high α). However, swelling in the bentonite was found to develop
 196 more slowly (low β).

197 Anticipated future work will look at empirical relationships between α and β and various
 198 drilling fluid compositional characteristics, with a view that these can be used to simulate drilling
 199 fluid improvements on oil-reservoir scale models of clay swelling phenomena.

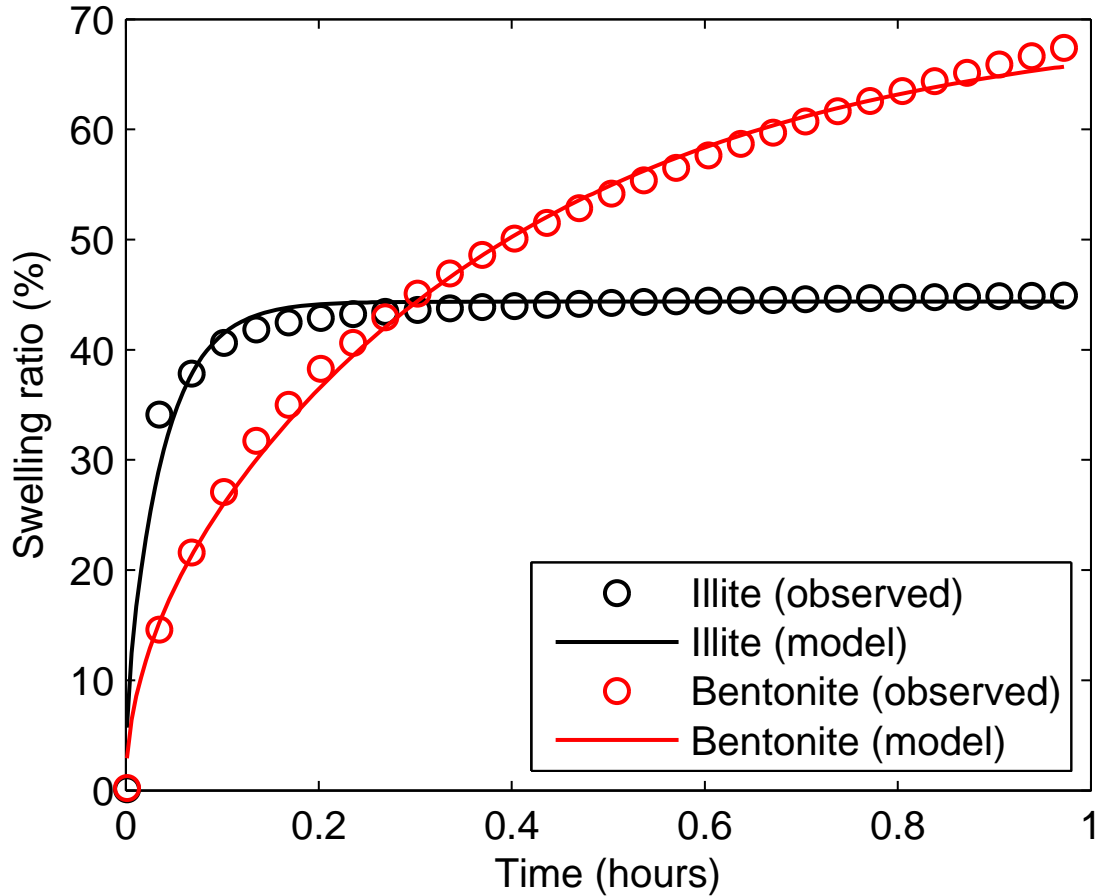


Figure 1: Plots of swelling ratio against time as observed during the experiments and as simulated from the calibrated models, according to Eq. (18).

200 **5. Acknowledgements**

201 We are very grateful for the useful comments provided by Peter Raats.

202 **6. References**

203 Anderson, R. L., Ratcliffe, I., Greenwell, H. C., Williams, P. A., Cliffe, S., Coveney, P. V. (2010). Clay swelling – A
 204 challenge in the oilfield. *Earth-Science Reviews*, 98, 201–216.

205 Chai, Z. Y., Kang, T. H., Feng, G. R. (2014). Effect of aqueous solution chemistry on the swelling of clayey rock.
 206 *Applied Clay Science*, 93, 12-16.

207 Chavali, R. V. P., Vindula, S. K., Babu, A., Pillai, R. J. (2017). Swelling behavior of kaolinitic clays contaminated
208 with alkali solutions: A micro-level study. *Applied Clay Science*, 135, 575-582.

209 Chen, Y. G., Zhu, C. M., Ye, W. M., Cui, Y. J., Chen, B. (2016). Effects of solution concentration and vertical stress
210 on the swelling behavior of compacted GMZ01 bentonite. *Applied Clay Science*, 124, 11–20.

211 Chertkov, V. Y. (2012). Physical modeling of the soil swelling curve vs. the shrinkage curve. *Adv. Water Resour.*, 44,
212 66–84.

213 Crank, J. (1975). *The Mathematics of Diffusion*: 2nd Ed. Clarendon Press.

214 Eriksen, T. E., Jansson, M., Molera, M. (1999). Sorption effects on cation diffusion in compacted bentonite. *Engineer-
215 ing Geology*, 54, 231–236.

216 Kim, D. J., Jaramillo, R. A., Vauclin, M., Feyen, J., Choi, S. I. (1999). Modeling of soil deformation and water flow
217 in a swelling soil. *Geoderma*, 92, 217–238.

218 Komine, H., Ogata, N. (1994). Experimental study on swelling characteristics of compacted bentonite. *Canadian
219 Geotechnical Journal*, 31, 478–490.

220 Oren, A. H., Akar, R. C. (2017). Swelling and hydraulic conductivity of bentonites permeated with landfill leachates.
221 *Applied Clay Science*, 142, 81–89.

222 Peng, X., Horn, R. (2007). Anisotropic shrinkage and swelling of some organic and inorganic soils. *Eur. J. Soil Sci.*,
223 58, 98–107.

224 Philip, J. R. (1969). Hydrostatics and hydrodynamics in swelling soils. *Water Resour. Res.*, 5, 1070–1077.

225 Raats, P. A. C. (2002). Flow of water in rigid and non-rigid, saturated and unsaturated soils. In: *The Modeling and
226 Mechanics of Granular and Porous Materials* edited by G. Capriz, V. N. Ghionna and P. Giovine, in the series
227 *Modeling and Simulation in Science, Engineering and Technology Series* edited by N. Bellomo, pp.181–210.

228 Santarelli, F. J., Carminati, S. (1995). Do shales swell? A critical review of available evidence. In *SPE/IADC Drilling
229 Conference*. Society of Petroleum Engineers.

230 Sellick, C., Underwood, T. R., Erdogan, A. R., Patel, R., Skipper, N., Greenwell, H. C. (2017). Assessing compacted
231 bentonite swelling in organic solvents using a non-contact linear swellometer. *Applied Clay Science*, In preparation.

232 Smalley, M. V. (2006). *Clay swelling and colloid stability*. CRC Press.

- 233 Smiles, D.E., Raats, P.A.C., (2005). Hydrology of swelling clay soils. In: Anderson, M.G. (Ed.), Encyclopedia of
234 Hydrological Sciences. Wiley, 1011–1026 (Chapter 67).
- 235 Song, X., and Borja, R. I. (2014). Mathematical framework for unsaturated flow in the finite deformation range. Int.
236 J. Num. Meth. Eng., 97, 658–682.
- 237 Su, N. (2010). Theory of infiltration: Infiltration into swelling soils in a material coordinate. J. Hydrol., 395, 103–108.
- 238 Suter, J. L., Coveney, P. V., Anderson, R. L., Greenwell, H. C., Cliffe, S. (2011). Rule based design of clay-swelling
239 inhibitors. Energy & Environmental Science, 4, 4572–4586.
- 240 Suter, J. L., Groen, D., Coveney, P. V. (2015). Chemically Specific Multiscale Modeling of ClayPolymer Nanocom-
241 posites Reveals Intercalation Dynamics, Tactoid Self-Assembly and Emergent Materials Properties. Advanced
242 Materials, 27, 966–984.
- 243 Van Oort, E. (2003). On the physical and chemical stability of shales. J. Pet. Sci. Eng., 38, 213–235.
- 244 Wilson, M. J., Wilson, L. (2014). Clay mineralogy and shale instability: an alternative conceptual analysis. Clay
245 Minerals, 49, 127–145.